

**Report for exercise 4 from group C**

Tasks addressed: 5

Authors:  
Alejandro Hernandez Artiles (03785345)  
Pavel Sindelar (03785154)  
Haoxiang Yang (03767758)  
Jianfeng Yue (03765255)  
Leonhard Chen (03711258)

Last compiled: 2024-03-02

Source code: <https://github.com/alejandrorhdez00/Exercises-MLCMS-Group-C/tree/main/Exercise-4>

The work on tasks was divided in the following way:

Alejandro Hernandez Artiles (03785345)	Task 1	20%
	Task 2	20%
	Task 3	20%
	Task 4	20%
	Task 5	20%
Pavel Sindelar (03785154)	Task 1	20%
	Task 2	20%
	Task 3	20%
	Task 4	20%
	Task 5	20%
Haoxiang Yang (03767758)	Task 1	20%
	Task 2	20%
	Task 3	20%
	Task 4	20%
	Task 5	20%
Jianfeng Yue (03765255) ( <b>Project Lead</b> )	Task 1	20%
	Task 2	20%
	Task 3	20%
	Task 4	20%
	Task 5	20%
Leonhard Chen (03711258)	Task 1	20%
	Task 2	20%
	Task 3	20%
	Task 4	20%
	Task 5	20%

## Report on task 1, Vector fields, orbits, and visualization

For the simulations in this task we use the provided function. Experimental results are used in visualization and analytical results are used to derive types of equilibria.

The plots are obtained using `task1/linear_1_parameter.ipynb`, whereas some plotting utilities are in `task1/linear_plotter.py`. Task 1, 2 and 3 also use `utils.py` for more general plotting utilities.

Firstly, for any eigenvalue it holds that

$$\|A - \lambda I\| = 0$$

for 2x2 matrix

$$(a - \lambda)(d - \lambda) - bc = 0$$

for our matrix  $a = b = \alpha$   $c = -4^{-1}$   $d = 0$

$$(\alpha - \lambda)(-\lambda) - (-4^{-1}\alpha) = 0$$

$$-\alpha\lambda + \lambda^2 + 4^{-1}\alpha = 0$$

whose solutions are

$$(\alpha \pm \sqrt{\alpha^2 - \alpha})2^{-1}$$

Because  $dy = -x/4$  the only point where  $dy = 0$  has to be  $x = 0$ .

$$dy = 0 \Rightarrow x = 0$$

$$x = 0 \wedge dx = \alpha y + \alpha x \Rightarrow dx = \alpha y$$

and therefore the only equilibrium for  $\alpha \neq 0$  is  $(0,0)$ . For  $\alpha = 0$  points  $\{(0,t), t \in R\}$  are equilibria.

At  $\alpha = 0$  the equilibria is unstable as if we start at any point that is not an equilibrium we go to positive or negative infinity.

For the other cases we must examine the eigenvalues of A, these are

$$(\alpha + \sqrt{\alpha^2 - \alpha})2^{-1}, (\alpha - \sqrt{\alpha^2 - \alpha})2^{-1}$$

This has no purely imaginary solutions. It has real solutions for  $\alpha^2 >= \alpha$  so for  $\alpha \in R - (0, 1)$ . It has imaginary solutions for  $\alpha \in (0, 1)$ . The imaginary part of the two solutions is always complementary.

For  $\alpha < 0$  one eigenvalue is positive and the other negative because

$$\sqrt{\alpha^2 - \alpha} \geq \alpha$$

So for  $\alpha < 0$  there will be a saddle at the point  $(0,0)$ .

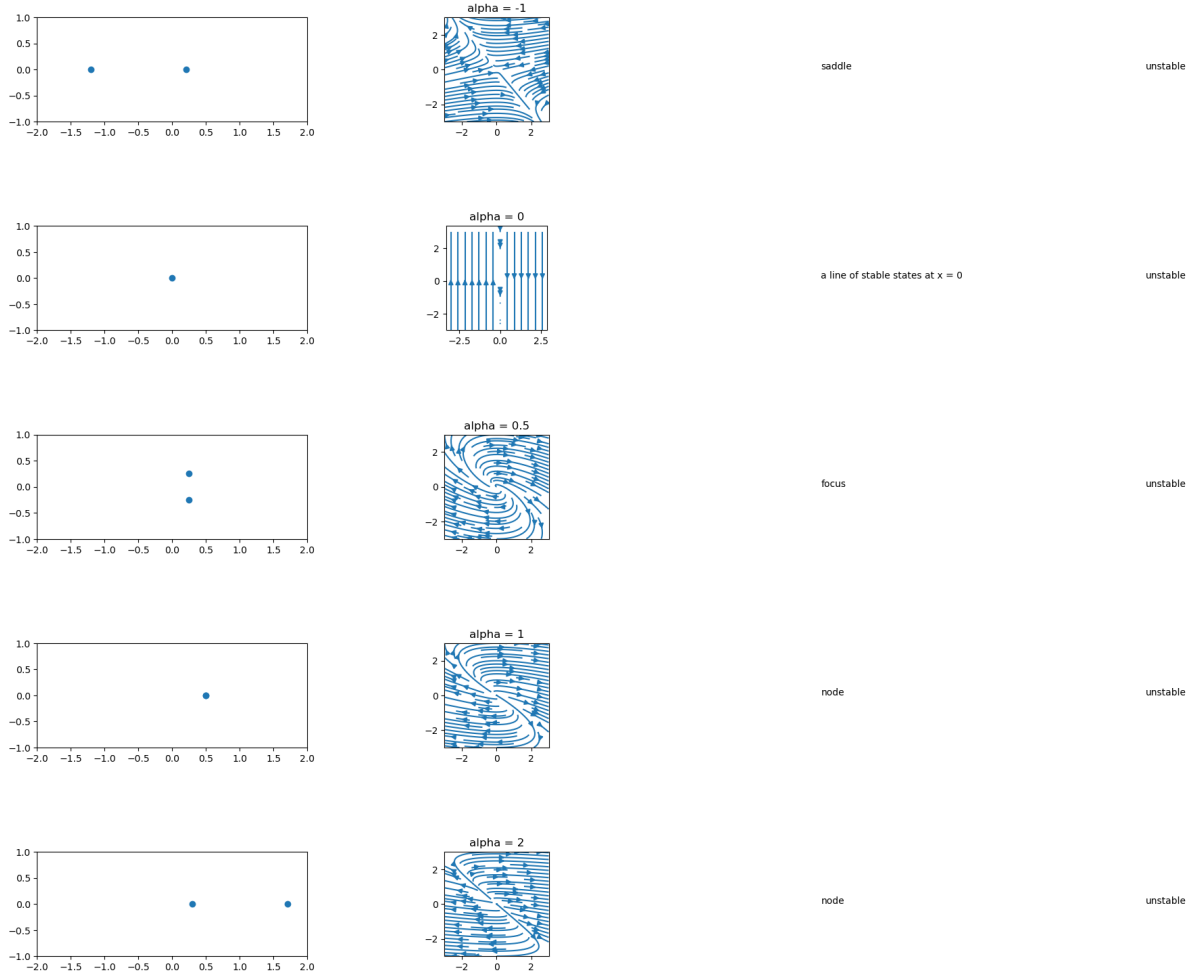
The eigenvalues real part is positive or zero for  $\alpha > 0$  because

$$\alpha \geq \text{real}(\sqrt{\alpha^2 - \alpha}) \geq 0$$

For the  $\alpha \geq 1$  this is trivial and because  $\text{real}(\sqrt{x}) = 0 \forall x < 0$  it holds also for  $\alpha \in (0, 1)$ .

If we also take into consideration that the solution is real for  $\alpha \geq 1$  that means that there will be an unstable node for this range at the point  $(0,0)$ .

Since the solution is imaginary for  $\alpha \in (0, 1)$ . The real part is the same for both because  $\text{real}(\sqrt{x}) = 0 \forall x < 0$  and the imaginary parts are complementary to each other because  $\text{im}(\alpha) = 0$ . that means that there will be an unstable focus for this range at the point  $(0,0)$ .

Figure 1: Phase diagrams of the system  $A_\alpha$  at different values of  $\alpha$ 

To be able to get all the types of equilibria (ie. the missing stable node and stable focus) we need to construct a matrix with eigenvalues with negative real parts. Imaginary eigenvalues at some  $\alpha$  and real eigenvalues at other  $\alpha$ .

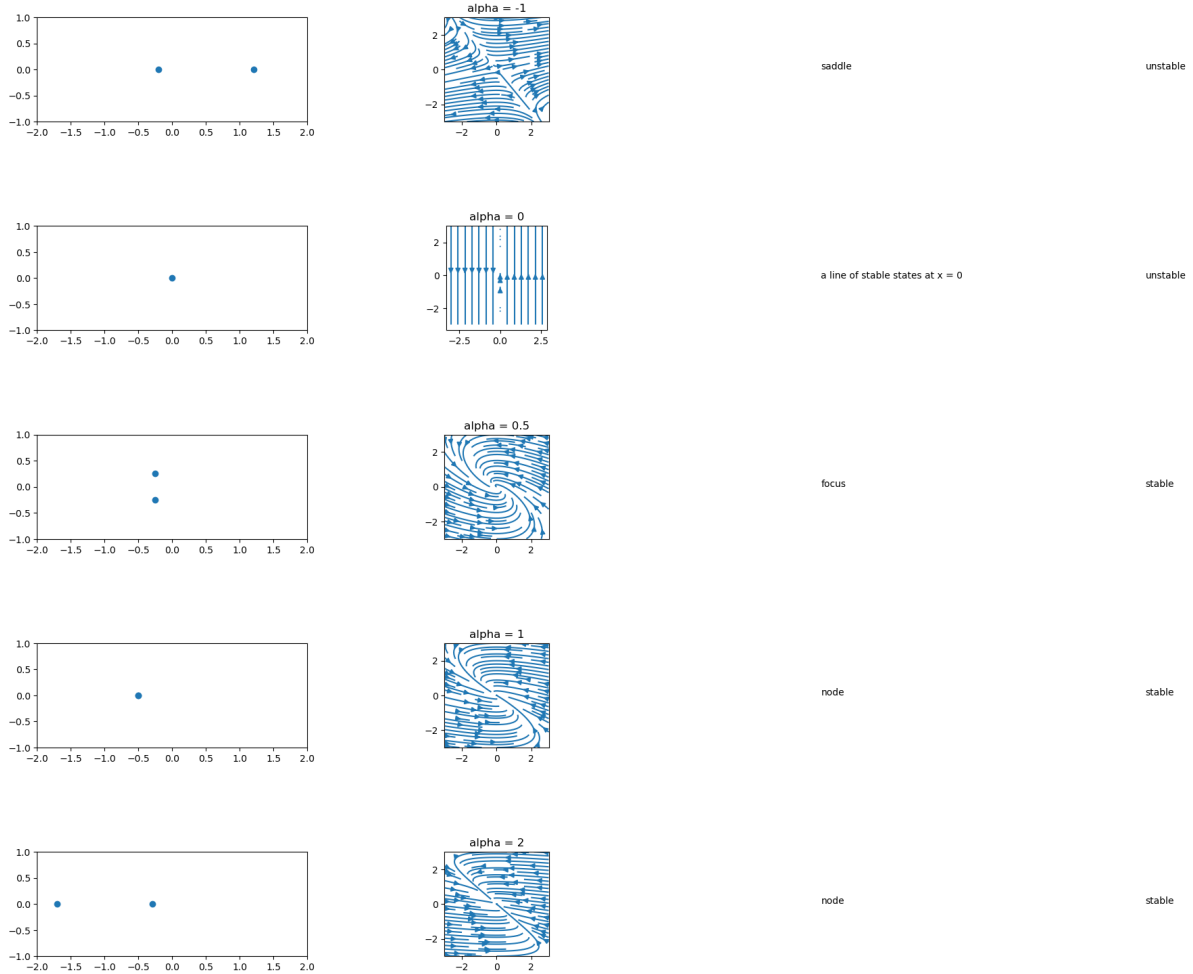
$$B_\alpha = \begin{bmatrix} -\alpha & -\alpha \\ \frac{1}{4} & 0 \end{bmatrix}$$

For  $\alpha = 0$  there will once again be a line of stable states at  $\alpha = 0$  and all other points will go toward negative or positive infinity in the second dimension and keep their first dimension.

For such a matrix's eigenvalues at other values of  $\alpha$  a similar equation holds as for  $A_\alpha$ .

$$\begin{aligned} \alpha\lambda + \lambda^2 + 4^{-1}\alpha &= 0 \\ (-\alpha - \sqrt{\alpha^2 - \alpha})2^{-1}, (-\alpha + \sqrt{\alpha^2 - \alpha})2^{-1} \end{aligned}$$

For  $\alpha \in (0, 1)$  the result will be two complementary imaginary values with negative real part so there will be an attractive focus equilibrium. For  $\alpha > 1$  the result will be two negative values so there will be an attractive node equilibrium. For  $\alpha < 1$  the result will be one negative and one positive value so there will be a saddle equilibrium.

Figure 2: Phase diagrams of the system  $B_\alpha$  at different values of  $\alpha$ 

And finally we can use these systems to reconstruct the figure from Kuznetsov 3.

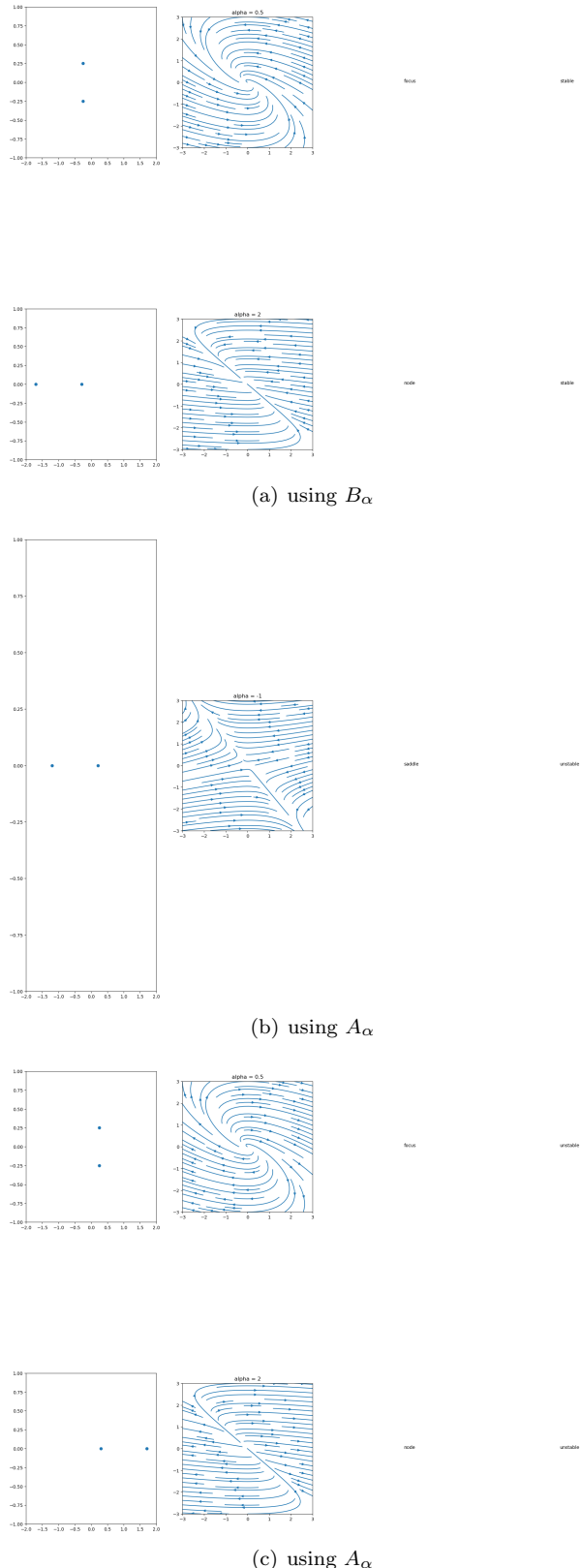


Figure 3: Topological classification of different equilibria on the plane.

Systems with nodes and focus positioned identically and possessing the same stability will be topologically equivalent. In Figure 3, this equivalence holds between the first and second systems, as well as between the

second-to-last and last systems. However, all other pairs are not topologically equivalent.

---

## Report on task 2, Common bifurcations in nonlinear systems

The solution and plots for this tasks are produced in `task2/non_linear_1_d.ipynb`. In addition, some specific plotting utilities are implemented in `task2/ode_d_plotter.py`.

In this task we will compare these equations defining parameterized dynamical systems on  $\mathbb{R}$ .

System 1

$$\dot{x}_1(x) = \alpha - x^2$$

System 2

$$\dot{x}_2(x) = \alpha - 2x^2 - 3$$

We can get the equilibria for  $\alpha - x^2$  by looking at the equation

$$\alpha - x^2 = 0$$

. This equation has roots

$$x = \pm\sqrt{\alpha}$$

so for  $\alpha < 0$  there will be no equilibria at  $\alpha = 0$  there will be one at  $x = 0$  and for  $\alpha > 0$  they will be  $x = \pm\sqrt{\alpha}$ .

For a set  $\alpha$  an equilibrium  $y$  is stable if  $\dot{x}$  at the interval around it has the opposite sign as  $x - y$ .

Because  $\alpha - x^2$  is a quadratic equation it has three intervals with different signs. It is negative at

$$x \in (-\infty, -\sqrt{\alpha})$$

positive at

$$x \in (-\sqrt{\alpha}, \sqrt{\alpha})$$

and negative again at

$$x \in (\sqrt{\alpha}, \infty).$$

For the special case  $\alpha = 0$  we can express the requirement as  $-x^2 < 0$  which does not hold for  $x < 0$  so the equilibrium is unstable.

When looking at  $\alpha > 0$  we see the following about the equilibria.

We write the requirement for  $y = \sqrt{\alpha}$

$$\begin{aligned} \alpha - x^2 &< 0 \wedge x - \sqrt{\alpha} > 0 \Leftrightarrow x > \sqrt{\alpha} \\ \alpha &> x^2 \wedge x < \sqrt{\alpha} \Leftrightarrow x \in (-\sqrt{\alpha}, \sqrt{\alpha}). \end{aligned}$$

From this we can see that the equilibrium at  $x = \sqrt{\alpha}$  is next to two intervals for which the requirement holds

$$x > \sqrt{\alpha}$$

and

$$x \in (-\sqrt{\alpha}, \sqrt{\alpha}).$$

We write the requirement for  $y = -\sqrt{\alpha}$

$$\begin{aligned} \alpha &< x^2 \wedge x > -\sqrt{\alpha} \Leftrightarrow x > \sqrt{\alpha} \\ \alpha &> x^2 \wedge x < -\sqrt{\alpha} \Leftrightarrow \perp. \end{aligned}$$

We can see that the equilibrium at  $x = -\sqrt{\alpha}$  is next to two intervals for which the requirement does not hold

$$x \in (-\sqrt{\alpha}, \sqrt{\alpha})$$

and

$$x < -\sqrt{\alpha}.$$

From these we can construct the bifurcation diagram by plotting the functions  $\sqrt{\alpha}$  and  $-\sqrt{\alpha}$ .

The first parameterized system undergoes a saddle-node bifurcation at  $\alpha = 0$  this is obvious from the telltale fork in the diagram in part a of the Figure 8 and of course from the fact that the equation is the normal form of the saddle-node bifurcation.

To construct example trajectories we use points that are in intervals of different signs for both polynomials at both values of  $\alpha$ . We then calculate the endpoint of the trajectory after simulating using `scipy.integrate.solve_ivp`

and draw an arrow from the starting point to the endpoint. This is valid because if the value diverges the arrow will point towards the divergence and if it converges it will point towards the convergence, a stable orbit is impossible in the given systems.

$$\alpha = 1$$

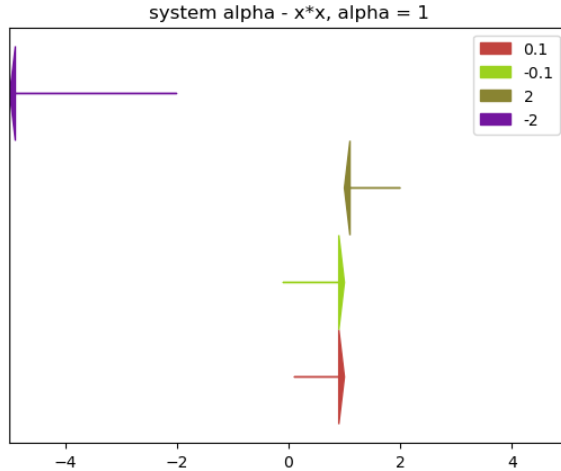


Figure 4: System 1 at  $\alpha = 1$  the color indicates the starting coordinate in  $\mathbb{R}$  (see legend).

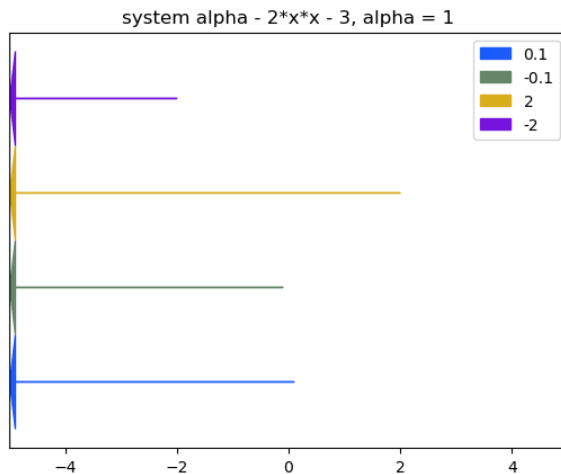


Figure 5: System 2 at  $\alpha = 1$  the color indicates the starting coordinate in  $\mathbb{R}$  (see legend).

and therefore System 1 at  $\alpha = 1$  has stable states

$$1 - x^2 = 0 \\ x = 1, x = -1$$

$$1 - 2x^2 - 3 = 0 \\ 2x^2 = -2$$

has no real solutions and therefore System 1 at  $\alpha = 1$  has stable states has no stable states

Any homeomorphism proving topologically equivalence is required to map orbits of one system onto orbits of another system. System 1 at  $\alpha = 1$  and System 2 at  $\alpha = 1$  are therefore not topologically equivalent because there is no way to map an empty set of orbits onto a non empty set or vice versa.

$$\alpha = -1$$

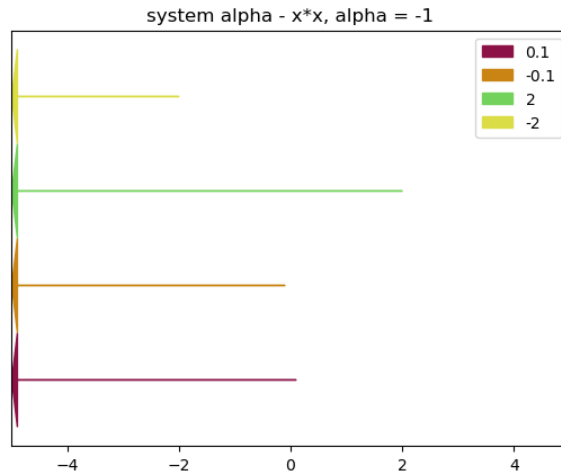


Figure 6: System 1 at  $\alpha = -1$  the color indicates the starting coordinate in  $\mathbb{R}$  (see legend).

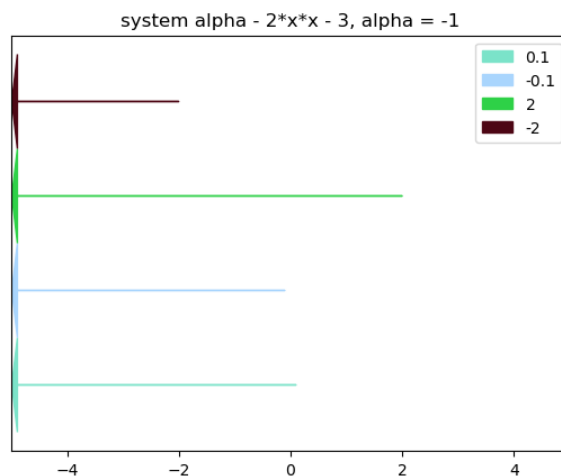


Figure 7: System 2 at  $\alpha = -1$  the color indicates the starting coordinate in  $\mathbb{R}$  (see legend).

The polynomial

$$-1 - x^2 = 0$$

has no real solution

$$x^2 = -1$$

and therefore System 1 at  $\alpha = -1$  has no stable points.

The polynomial

$$-1 - 2x^2 - 3 = 0$$

$$2x^2 = -4$$

has no real solutions and therefore System 2 at  $\alpha = -1$  has no stable points.

System 1 at  $\alpha = -1$  and System 2 at  $\alpha = -1$  are topologically equivalent because if we take the identity mapping on  $\mathbb{R}$  this mapping is bijective and continuous (it's inverse is equal to it and therefore also continuous) and it maps the empty set of orbits of System 1 at  $\alpha = -1$  onto the empty set of orbits of System 2 at  $\alpha = -1$ .

Looking at figures in 8 we can see that both systems undergo one bifurcation. We can also see that before then the systems have no stable points. Afterwards they have one stable and one unstable point, these are the defining characteristics of the one-dimensional saddle-node bifurcation. This is an argument as to why these parametrized systems have the same normal form as all parametrized systems that undergo the same bifurcations have the same normal form.

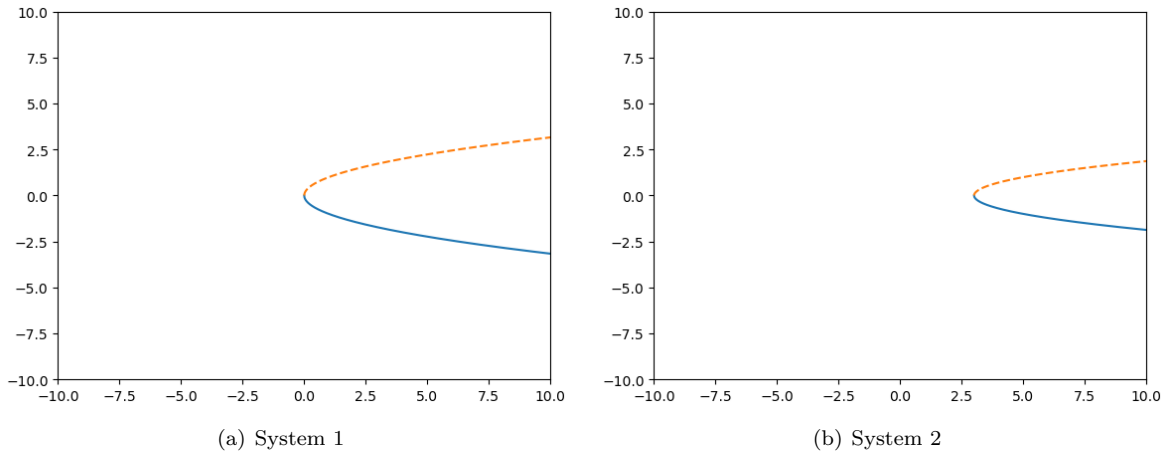


Figure 8: The x coordinate indicates the  $\alpha$ , the y coordinate of the dotted curves indicates the coordinate in  $\mathbb{R}$  of the stable equilibrium and the y coordinate of the full curves indicates the coordinate in  $\mathbb{R}$  of the unstable equilibrium

### Report on task 3, Bifurcations in higher dimensions

The solution and plots for this task can be found in `task3/non_linear_2_d.ipynb` for the first equation and in `task3/non_linear_2_params.ipynb` for the second equation. Finally, some specific plotting utilities are implemented in `task3/zero_convergence_plotter.py` by means of the `ZeroConvergencePlotter` class.

This task mostly concerns visualizing things. The task was accomplished using two python notebooks. For the visualization of the orbits it was decided to use the `scipy.integrate.solve_ivp` solver.

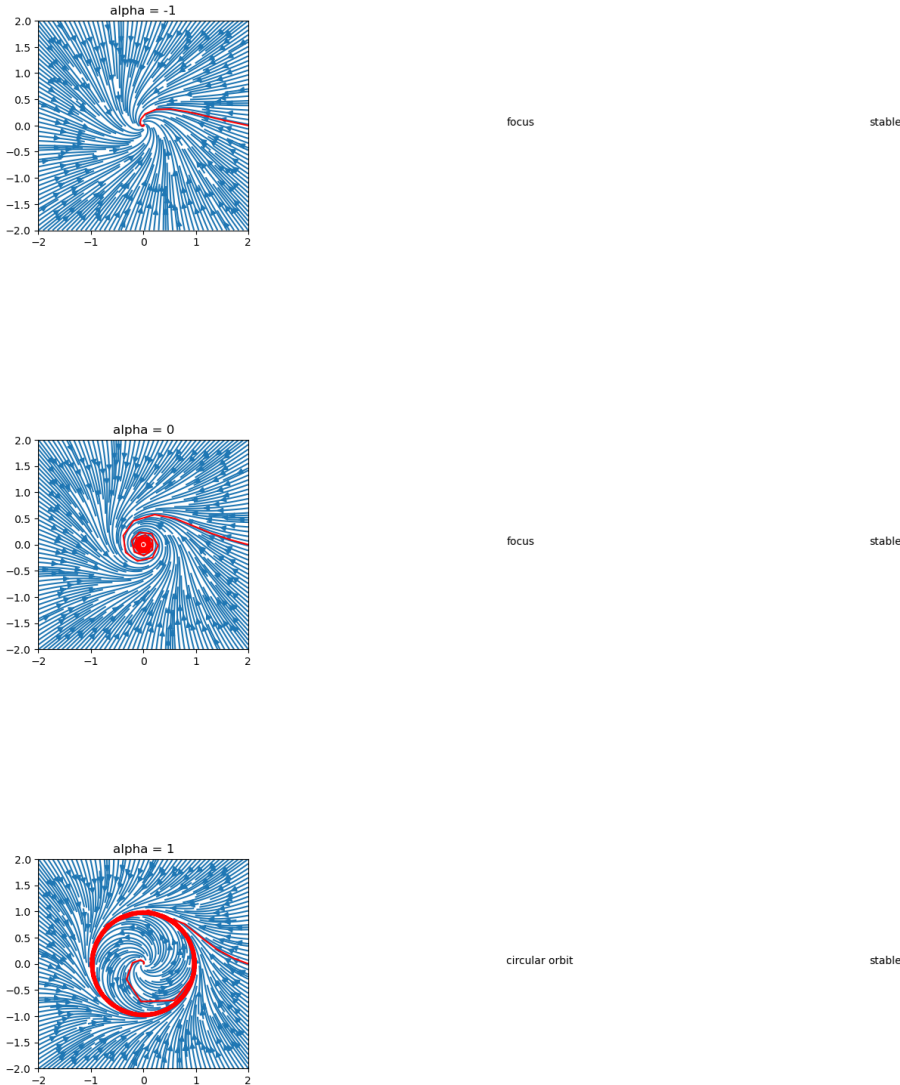
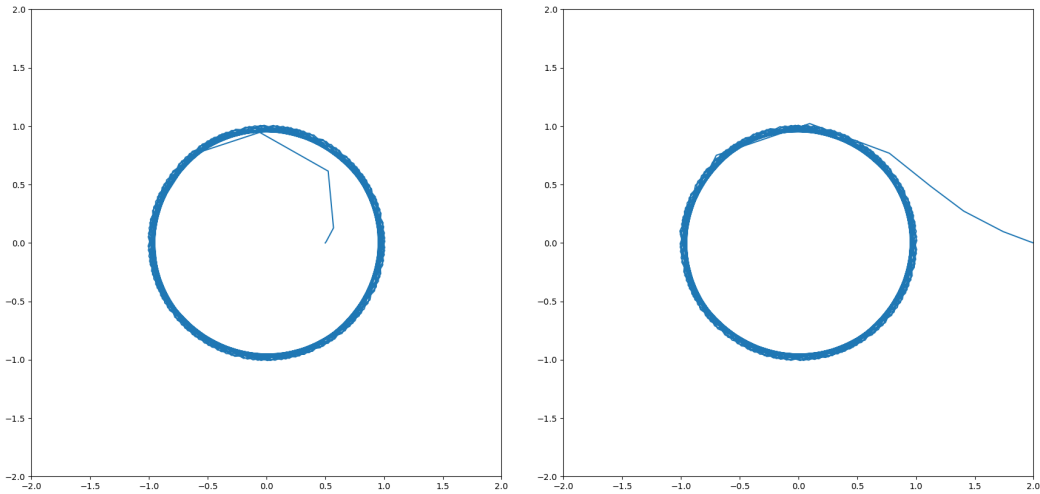


Figure 9: Phase diagrams of the system at different values.

We can see in Figure 9 that the systems at  $\alpha = -1$  and  $\alpha = 0$  simply have one stable focus at  $(0,0)$ . The system at  $\alpha = 1$  has a stable orbit at  $x^2 + y^2 = 1$ .



(a) the orbit that trajectory starting at  $(2, 0)$  settles into  
 (b) the orbit that trajectory starting at  $(0.5, 0)$  settles into

Figure 10: Orbits of the system for  $\alpha = 1$ .

We can see in Figure 10 that trajectories starting at both these points settle in the stable orbit at  $x^2 + y^2 = 1$ .

We can construct Figure 11 through the procedure outlined in the assignment. That is we sample  $(x, \alpha_2)$  uniformly and then plot the surface as a function  $\alpha_1 = -((\alpha_2)x - x^3)$ . We also plot a different plot where we sample  $(x, \alpha_2)$  and then take  $\alpha_1$  in steps of given size.

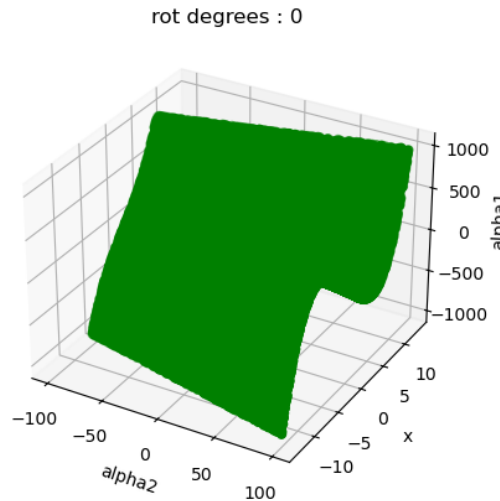


Figure 11: 3D plot of the bifurcation surface

The cusp cannot be seen in the diagram 11. It is called cusp bifurcation because in the parameter space we can separate the area where there are 3 equilibria from the area where there is only 1 equilibrium using two curves, these meet at the cusp point.

## Report on task 4, Chaotic dynamics

In this task we will explore two dynamical systems with chaotic behaviour, the logistic map, and the Lorenz system. Both systems are implemented in the `bifurcation.py` file and the plots are generated by `visualization.py`. All the experiments for this task can be found inside the folder "task4" in the notebook `experiments_task4.ipynb`.

Each of these systems have two functions inside `bifurcation.py`. The function that computes the system in an atomic level, and the simulation function that runs the previous function for a given time.

In addition, the logistic map has a `warmup` parameter to discard a certain number of initial iterations when simulating the logistic map. This is done to allow the system to reach a steady state before collecting data for the plot. Then, the `numttoplot` parameter is used to select the amount of final iterations to plot for each  $r$  value.

**Logistic map** The logistic map is defined as:

$$x_{n+1} = rx_n(1 - x_n), n \in \mathbb{N}$$

We will study how the system behaves depending on the value of  $r$ . When we vary the value of  $r$  from 0 to 2, we can see how for  $0 \leq r \leq 1$  the system has a stable fixed point at  $x = 0$ . For  $1 < r \leq 3$  the system converges to the stable fixed point  $x_s = \frac{(r-1)}{r}$  [7]. In Figure 12 we observe this behaviour only for  $1 < r \leq 2$ . We can observe how a period-doubling bifurcation occurs, i.e. a slight change in a system's parameters causes a new periodic trajectory to emerge from an existing periodic trajectory.

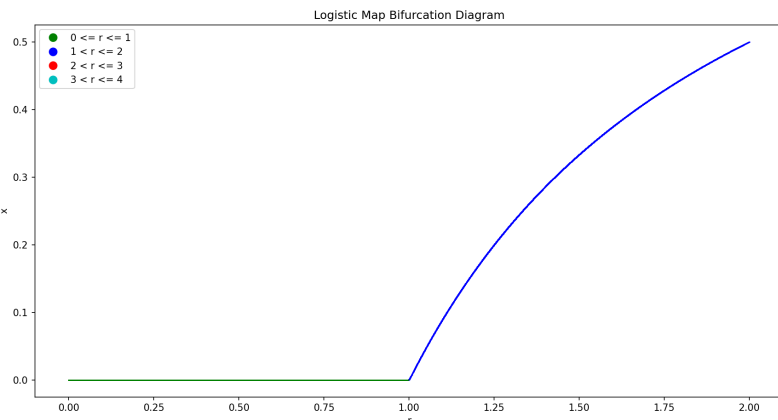
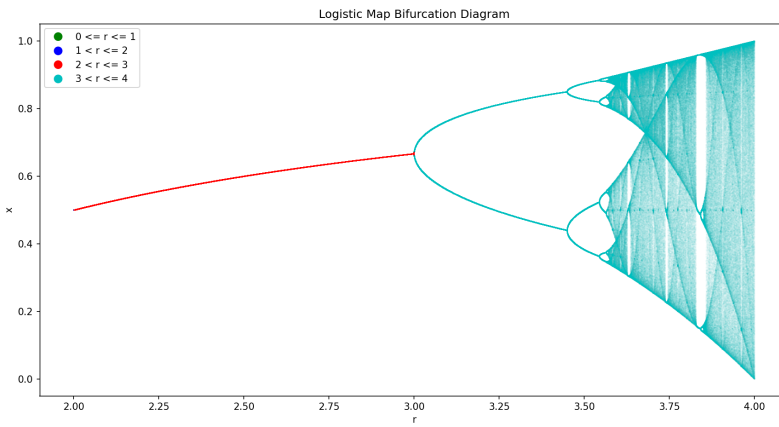
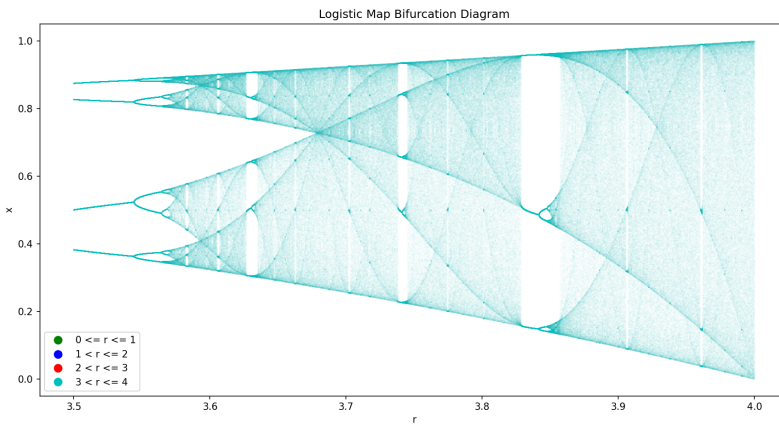


Figure 12: Logistic map  $r \in [0, 2]$

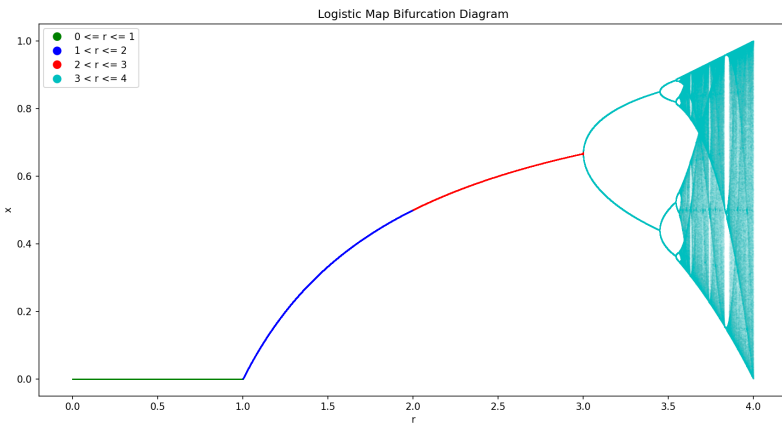
On the other hand, when we vary the value of  $r$  from 2 to 4, we can observe a distinct behaviour. As  $r$  continues to increase, subsequent period-doubling bifurcations occur, leading to stable orbits. However, when  $r$  is approximately greater than 3.57 the system undergoes a transition to chaos. This is a sudden and qualitative change in behavior characterized by aperiodic, apparently random dynamics. The system shows extremely high sensitivity to initial conditions, and its long-term behavior becomes unpredictable [1].

Figure 13: Logistic map  $r \in [2, 4]$ 

Moreover, if we look closely Figure 14 we can observe what appear to be stable regions within the chaotic region, i.e. we can find again period-doubling bifurcations inside the big gaps left by the chaotic trajectory.

Figure 14: Logistic map  $r \in [3.5, 4]$ 

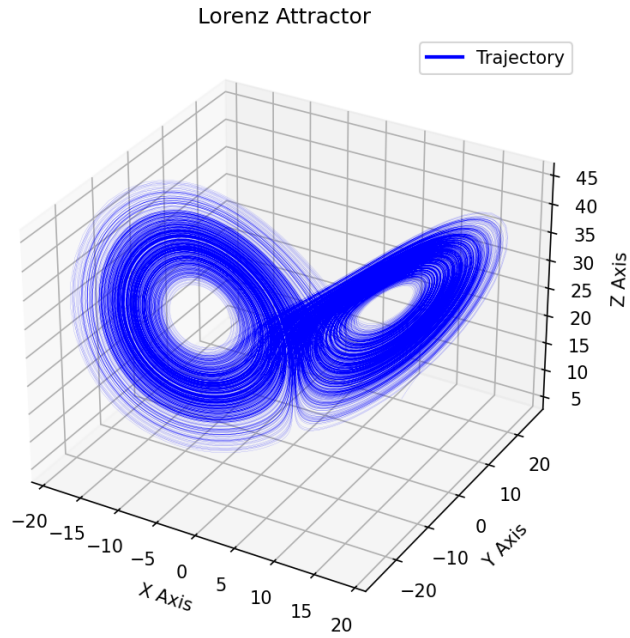
Finally, in Figure 15 we can observe the whole diagram for  $r \in [0, 4]$ . We can notice the stable fixed point at  $x = 0$  when  $0 \leq r \leq 1$ . For  $1 < r \leq 3$  we can observe the first period-doubling bifurcation. For  $r > 3$  this orbit continues to split in more period-doubling bifurcations until reaching the critical value we commented before, i.e.  $r \approx 3.57$ , when the chaotic behaviour starts, making the system unpredictable and very sensitive to initial conditions.

Figure 15: Logistic map  $r \in [0, 4]$ 

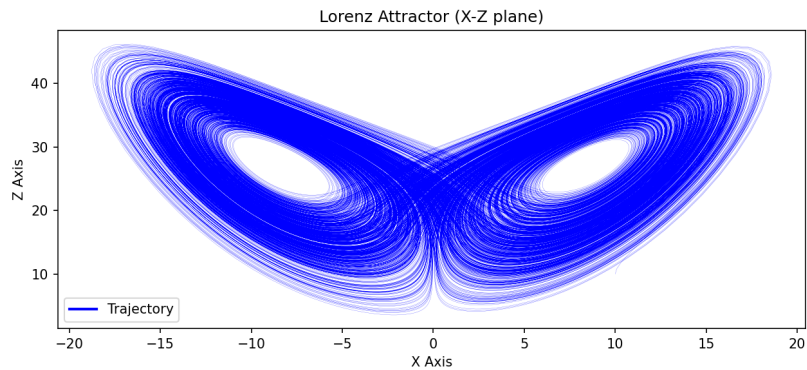
**Lorenz attractor** Now, we will study a system in three-dimensional space that exhibits chaotic behaviour, the Lorenz system. This system is given by the following equations [4]:

$$\begin{aligned} \frac{dx}{dt} &= \sigma(y - x) \\ \frac{dy}{dt} &= x(\rho - z) - y \\ \frac{dz}{dt} &= xy - \beta z \end{aligned}$$

To test the operation of the system, we will start by testing with some initial conditions  $x_0 = (10, 10, 10)$  and the parameter values  $\sigma = 10, \beta = 8/3, \rho = 28$  for a time  $T_{end} = 1000$ . In Figure 16 we can observe the trajectory generated by the system. The trajectory seems to oscillate between two hidden chaotic attractors, as well as a periodic attractor in point  $x = 0$ , where the trajectory always passes. The system appears to produce a chaotic trajectory for the given parameters, but we will test this checking its sensitivity to initial conditions.



(a) 3D plot



(b) XZ plane plot

Figure 16: Plots for  $\sigma = 10$ ,  $\beta = 8/3$ ,  $\rho = 28$ 

Therefore, now we will slightly perturb the initial conditions  $x_0$  to  $x_0 = (10 + 10^{-8}, 10, 10)$ . Now, we can check the difference between the trajectory with the original initial conditions and the perturbed one.

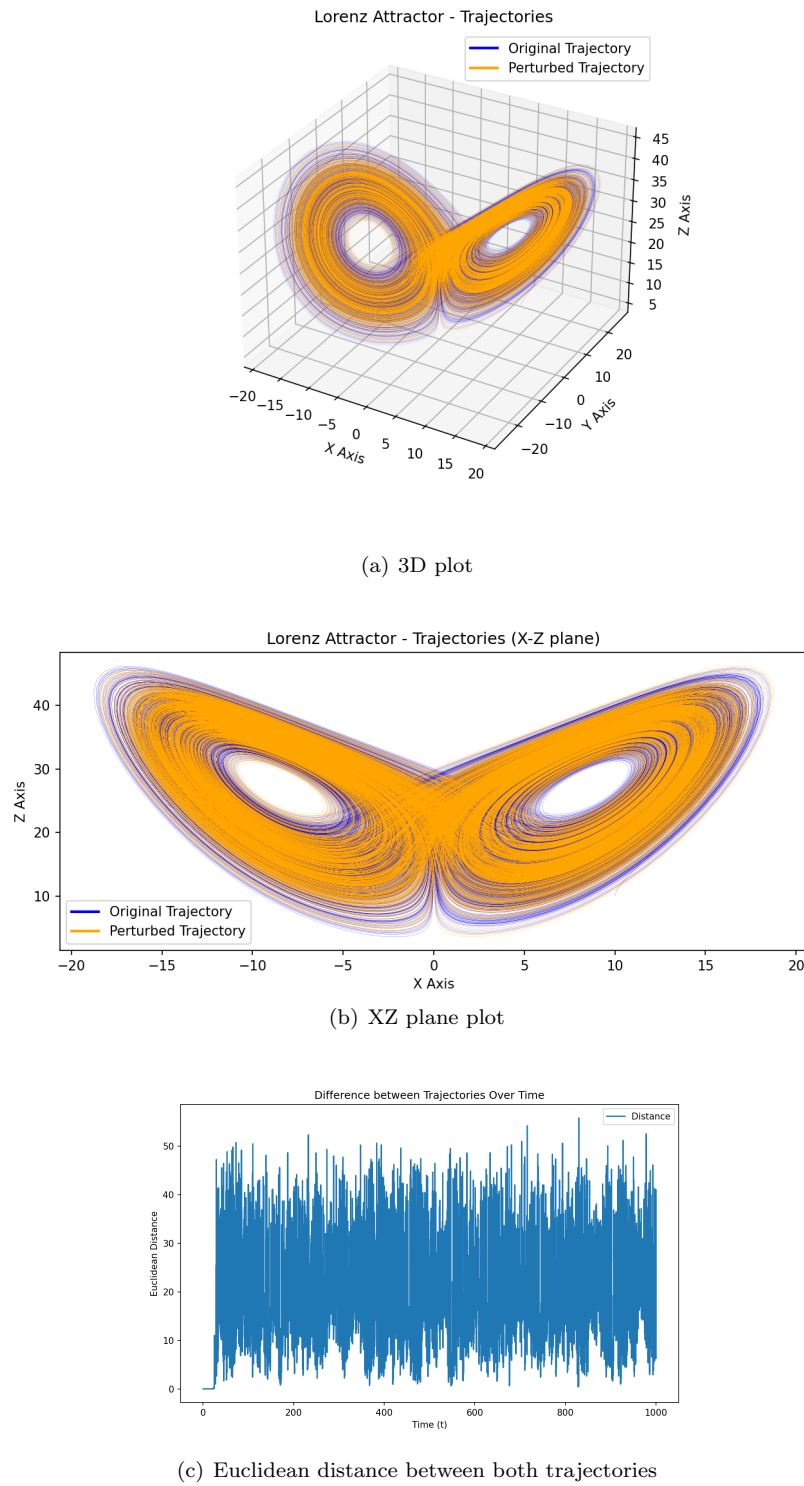


Figure 17: Comparison between the original and the perturbed trajectories

In Figure 17a and 17b we can observe that the overall structure of the trajectory is preserved by changing the initial conditions. However, analyzing Figure 17c we can check how the Euclidean distance between both trajectories explodes when reaching a certain value. Thus, we can verify that the behaviour of the system is chaotic, since varying the initial conditions by a minimum perturbation results in a trajectory that is very far from the original one. Although they keep the same structure, both trajectories are not the same.

It is also interesting to note that the distance has peaks but also troughs, which seem to be random, given the chaotic behaviour of the system. However, we also hypothesise that when the distance between the trajectories goes down it is because they are passing through the attractor located at  $x = 0$ , where all trajectories end up passing each time.

In order to analyze better when the distance between the trajectories starts to grow, we have run the system only for  $T_{end} = 30$ . Now, in Figure 18 we can observe how both trajectories are equal until approximately  $t = 23$  where we can note a small perturbation where the distance is greater than 0; however the crucial time is at  $t = 25$  when there is a sudden difference. After that, the distance between them explodes reaching a difference greater than 40 between both trajectories, exhibiting how the chaotic behaviour emerges exponentially fast.

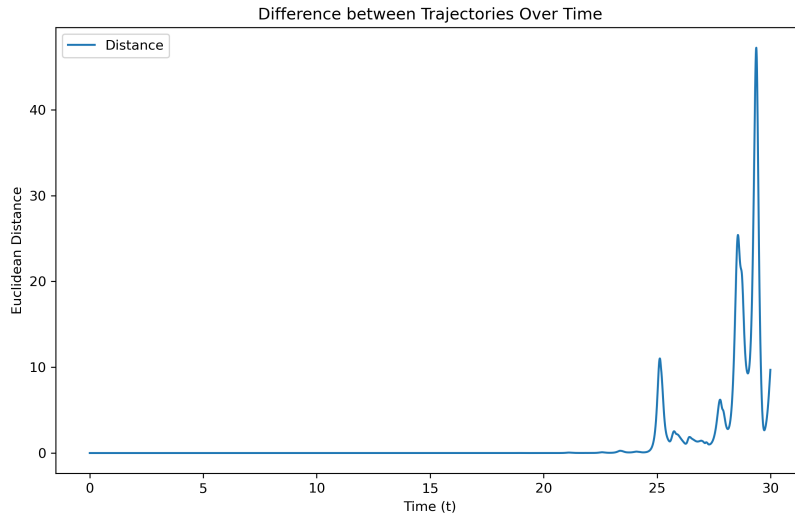
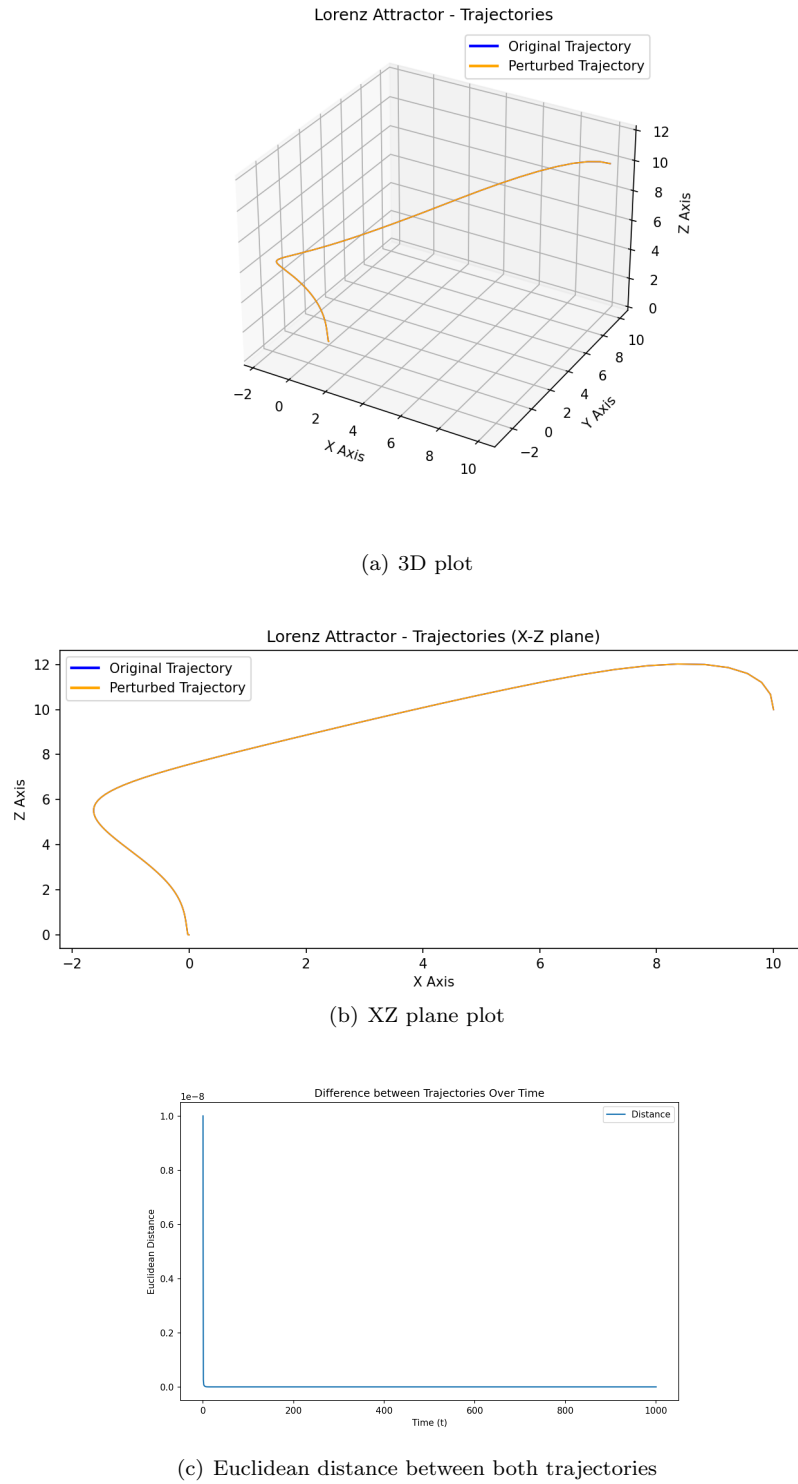


Figure 18: Distance for  $T_{end} = 30$

Now, given the same sets of initial conditions as before, we will check how changing the parameter  $\rho$  changes the system's behaviour. We first try  $\rho = 0.5$ , that can be observed in Figure 19. Now, it is clear that the system is not chaotic anymore. Both trajectories converge to the same point  $(0,0,0)$ , being their euclidean distance 0 for almost all the time, and its farthest point being at  $t = 0$ , where its distance is  $10^{-8}$ , the initial perturbation value added. Thus, the system is not chaotic with this parameter configuration, due to it not being sensitive to initial conditions and then being predictable.

Figure 19: Comparison for  $\rho = 0.5$ 

Also, we know that the Lorenz system is chaotic for  $(\sigma = 10, \beta = 8/3, \rho = 28)$  and nearby values [2]. Therefore, when trying other values for  $\rho$  like  $\rho = 5$  it is not surprising to see the same non-chaotic behaviour as before. We also increased the perturbed  $x_0$  to be  $x_0 = (10 + 5, 10, 10)$ . Again, in Figure 20 we can observe that the system is not chaotic, not being so sensitive to the initial conditions. Also, we can see better how both trajectories are being attracted by an attractor, executing a spiral trajectory. This also can be noted in Figure

20c, where the distance starts at 5, the perturbation value, and strictly decreases until it is 0.

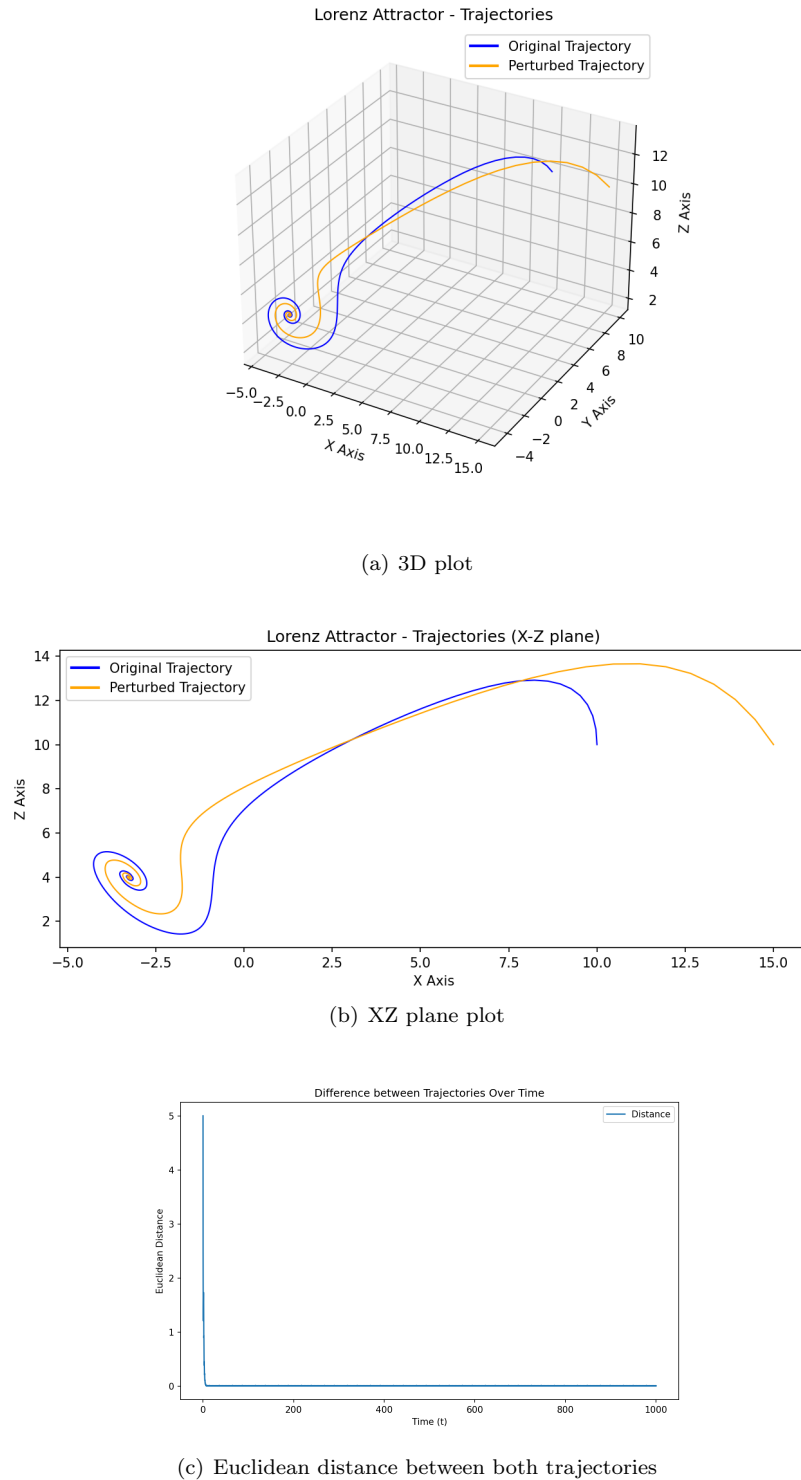


Figure 20: Comparison for  $\rho = 5$

Finally, we can answer the question: Is there a bifurcation (or multiple ones) between the value  $\rho = 0.5$  and  $\rho = 28$ ? Given the definition of a bifurcation: "The appearance of a topologically nonequivalent phase portrait under variation of parameters is called a bifurcation". Consequently, the question can be resolved by

determining whether the systems at these parameter values are topologically equivalent.

Looking at the corresponding Figures for each  $\rho$  value (Figure 16, 19) we can clearly see that there is no homeomorphism that maps the orbit of the system with  $\rho = 0.5$  to the system with  $\rho = 28$ . To elucidate, it becomes evident that no function can be found that effectively maps the predictable behavior of the first system to the extreme sensitivity to initial conditions exhibited by the latter system. Each infinitesimal change in the initial conditions of the latter system would necessitate a new mapping for the first one, precluding the identification of a unique map. This reasoning similarly applies to the comparison of systems with  $\rho = 5$  and  $\rho = 28$ .

---

## Report on task 5, Bifurcations in crowd dynamics

In this task we want to apply our knowledge about bifurcation theory to analyze and describe a given SIR model from [6]. Unless mentioned all tests were performed with the following values:

$$A = 20, d = 0.1, \nu = 1, \mu_0 = 10, \mu_1 = 10.45, \beta = 11.5, b = 0.022$$

**Task 5.1: Setup description** For this task `sir_model.py` and `sir_bed_model_unfinished.ipynb` were used as code framework. Apart from adding the needed documentation we decided to put the plotting from the python notebook into separate functions. These functions can be found in `sir_model_visualization.py`. This makes the code more readable and modular for later use when creating multiple plots of the SIR simulation.

**Task 5.2: Model implementation** Due to moving the plotting functions into a separate python file, the imports were moved as well. The python notebook only needs to import `sir_model_visualization`.

The differential equation based model from [6] was implemented according to the exercise sheet in the `model(...)` function in `sir_model.py`.

**Task 5.3: Experiments** In this task we are observing multiple graphs of the SIR simulation as well as its trajectories. For readability we only use a selected choice of plots, but a more extensive collection can be found in the python notebook `sir_bed_model-t5_3.ipynb`. For this we used different initial values  $(S_0, I_0, R_0)$  for the simulation. Here the  $S_0$  is the amount of susceptible,  $I_0$  the amount of infected and  $R_0$  the amount of removed people at  $t = 0$ . We tested with the following initial values.

$$(195.3, 0.052, 4.4), (195.7, 0.03, 3.92), (193, 0.08, 6.21)$$

We then observed the graphs for a diverse range of the variable  $b$ , which is the number of hospital beds per 10,000 persons [6]. We performed observations for  $b \in \{0.01, 0.03\}$  in increments of 0.001. By doing this we can observe a special kind of bifurcation.

In figure 21 we present a selected choice of the trajectories plotted in 3 dimensions. Here opaque plot lines in red were added. In figure 21(b) for  $b = 0.022$  we can observe a bifurcation. This is indicated by figure 21(a) and 21(c), where we observe the trajectories before and after this critical point and see 2 different trajectories for the systems stability. Corresponding to the trajectory for  $b = 0.022$  we see in figure 21(d) further plots.

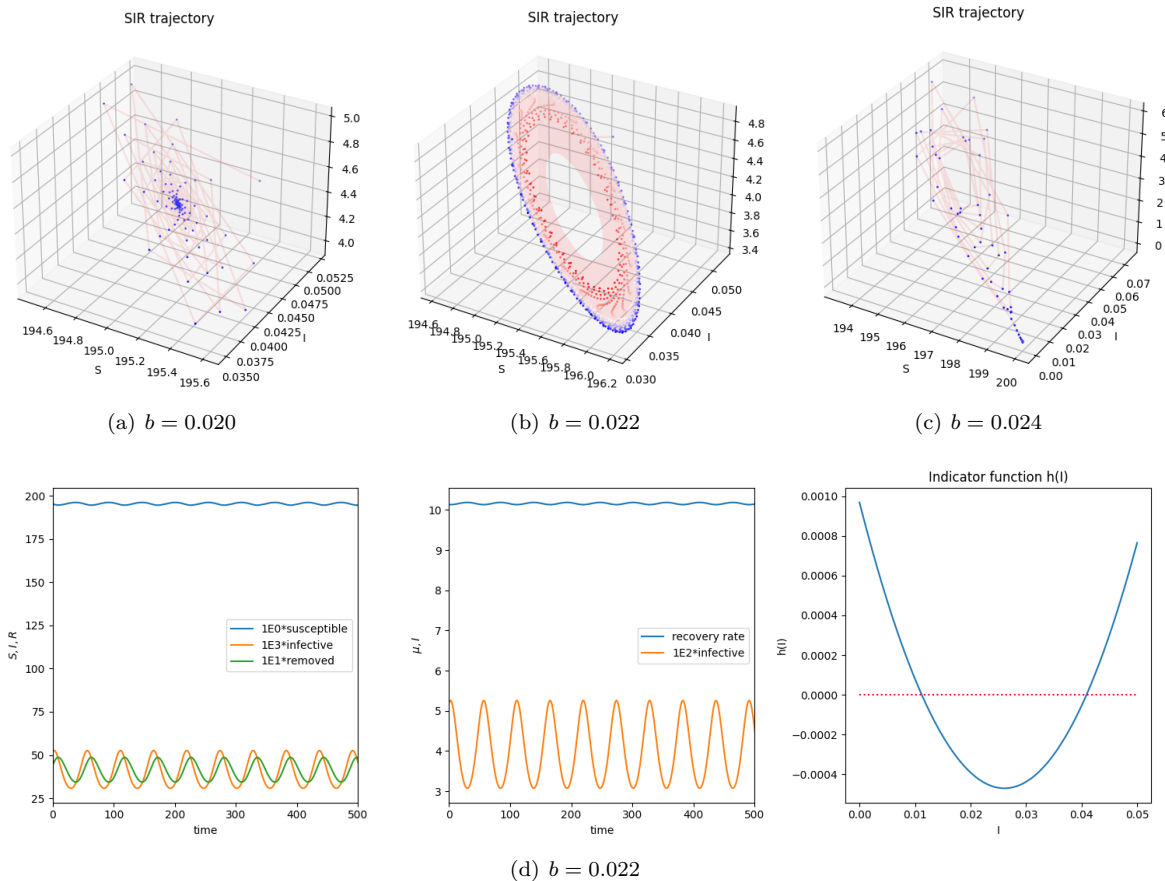
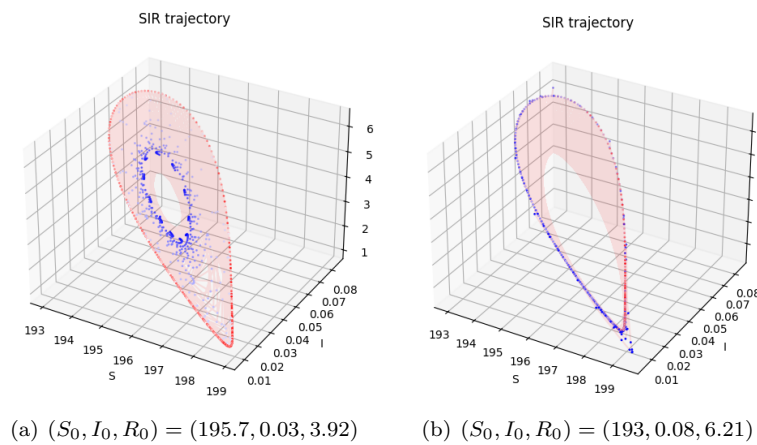
The first plot in 21(d) plots the  $S, I, R$  counts over time  $t$ . We can observe a periodic behaviour for these  $S, I, R$  counts over time. For  $b = 0.020$  we would observe a high amplitude at  $t = 0$  which decays over time. For  $b = 0.024$  we observe the opposite case with a small amplitude at  $t = 0$  which grows larger over time. For border cases with  $b = 0.01$  or  $b = 0.03$  we observe the periodic behaviour practically vanishing from the graph.

In the second plot of 21(d) we show recovery rate and infected counts plotted over time. Similar to the first plot we observe the same periodic behaviour. It is noteworthy that for  $b = 0.022$  we have seemingly a stable state where the plotted graphs behave like a periodic functions. Unlike this for  $b \neq 0.022$  the graphs instead reach a constant value over time  $t$ .

The last plot in figure 21(d) shows the indicator function  $h(I)$ . As described in [6] section 4.2 essentially  $h(I) = 0$  is a necessary condition for a Hopf bifurcation. We can observe  $h(I) = 0$  at two points. This function is defined as

$$\begin{aligned} c_0 &= b^2 d A \\ c_1 &= b((\mu_0 - \mu_1 + 2d)A + (\beta - \nu)b d) \\ c_2 &= (\mu_1 - \mu_0)b\nu + 2bd(\beta - \nu) + dA \\ c_3 &= d(\beta - \nu) \\ h(I) &= c_0 + c_1 I + c_2 I^2 + c_3 I^3 \end{aligned}$$

In figure 22(a) and (b) we see the trajectories of for the initial values  $(S_0, I_0, R_0) = (195.7, 0.03, 3.92)$  and  $(S_0, I_0, R_0) = (193, 0.08, 6.21)$  at  $b = 0.022$ . Their corresponding graphs are also showing the periodic behaviour we have observed in figure 21(d). We observe that for different starting values  $(S_0, I_0, R_0)$  the trajectories take a different form. Similar to the Hopf bifurcation in 21(b) we see blue and red dots in figures 22(a) and (b).

Figure 21: Plots for  $(S_0, I_0, R_0) = (195.3, 0.052, 4.4)$  and different  $b$ Figure 22: Plots for  $b = 0.022$  and other initial values  $(S_0, I_0, R_0)$

**Task 5.4** We observe the Hopf bifurcation at  $b = 0.022$ . From the abstract of [5] "a Hopf bifurcation occurs as a spiral point switches from stable to unstable (or vice versa) and a periodic solution appears". In Figures 21(a) to (c) we see a spiral point switch from stable to unstable state. We see the periodic solution in first 2 figures of 21(d). But also from [6] theorem 4.4 is proven i.e a generic Hopf bifurcation could occur. Then examples are provided as  $(195.3, 0.052, 4.4)$  spirals inward to a stable focus (see 21(b)),  $(195.3, 0.052, 4.4)$  spirals inward to the stable focus (see 22(a)) and  $(193, 0.08, 6.21)$  spirals inward to a stable limit cycle (see 22(b)).

From [3] page 84 the normal-form of the Hopf Bifurcation is defined as:

$$\begin{cases} \dot{x}_1 = \alpha x_1 - x_2 - x_1(x_1^2 + x_2^2), \\ \dot{x}_2 = x_1 + \alpha x_2 - x_2(x_1^2 + x_2^2) \end{cases}$$

But as evidenced from testing with different parameters we observed that the dynamical system is dependant more than 2 parameters. Looking into [6] section 4.3, it is also proven that the cusp type of Bogdanov–Takens bifurcation of codimension 3 occurs at  $E_*$ . In that section the prove of [6] theorem 4.7 leads us to the normal-form:

$$\begin{cases} \dot{X} = Y, \\ \dot{Y} = \epsilon_1 + \epsilon_2 Y + \epsilon_3 XY + X^2 - X^3Y + \mathcal{O}(|X, Y|^4)Y. \end{cases}$$

Here  $(\epsilon_1, \epsilon_2, \epsilon_3)$  are a function of the bifurcation parameters  $(\mu_1, b, \beta)$ .

**Task 5.5** From the implementation in `sir_model.py` and [6] we can draw the definition of the reproduction number  $\mathbb{R}_0$ . Here  $\beta$  is the average number of adequate contacts per unit time with infectious individuals.  $d$  is the per capita natural death rate.  $\nu$  is the per capita disease-induced death rate.  $\mu_1$  is the maximum recovery rates based on the number of available beds. The reproduction number is defined as the following:

$$\mathbb{R}_0 = \frac{\beta}{d + \nu + \mu_1}$$

Intuitively the reproduction rate  $\mathbb{R}_0$  is the ratio between the average contacts with infected individuals per unit time and maximal rate of removing individuals. Essentially the reproduction rate  $\mathbb{R}_0$  is the infection rate in relative to the (maximal) removal rate.

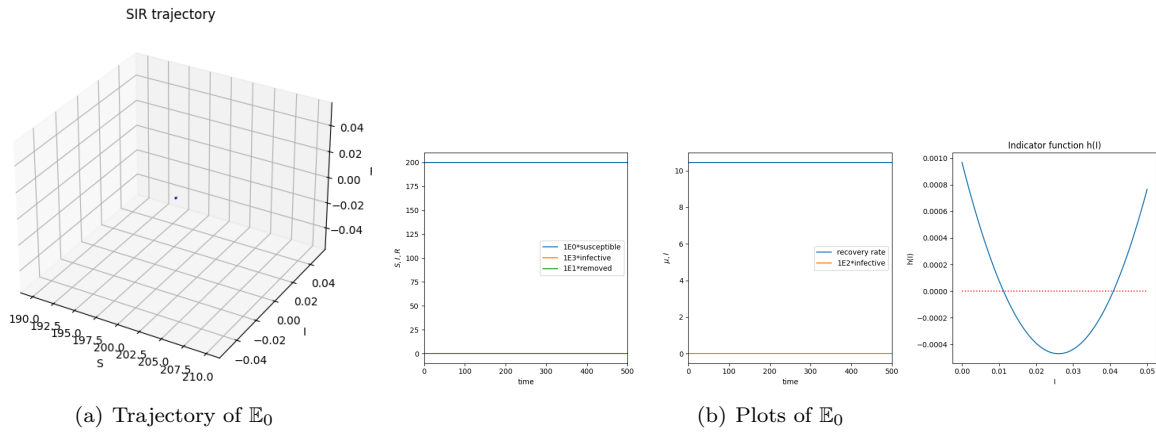
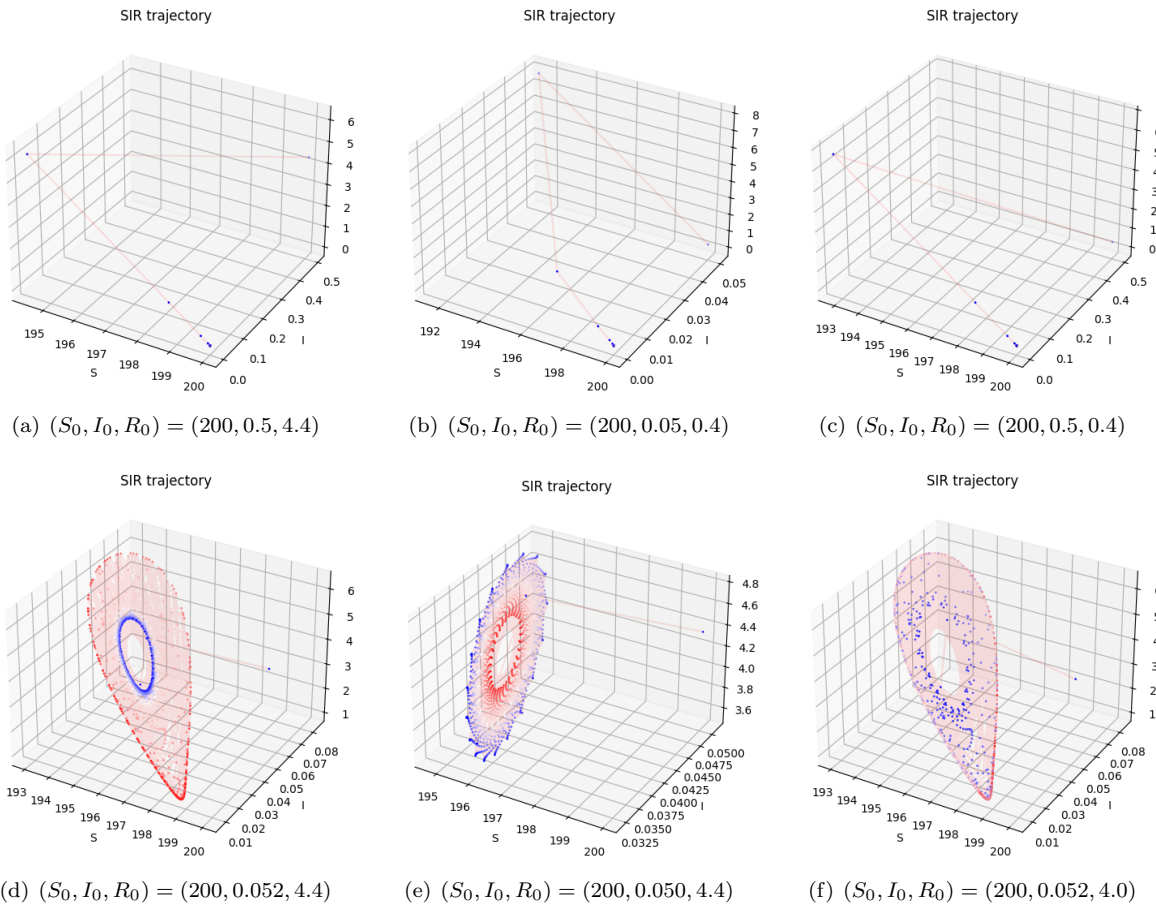
From [8] section 3 the reproduction number  $\mathbb{R}_0$  is cited as "the expected number of secondary cases produced, in a completely susceptible population, by a typical infective individual". Overall from [8] we can conclude that, if  $\beta$  increases or decreases the reproduction rate also increases or decreases. If the reproduction rate is  $\mathbb{R}_0 < 1$ , the infection can not grow. If  $\mathbb{R}_0 > 1$  holds, then each infected individual produces more than one new infection on average and hence the infection can spread.

In our previous observations in Figure 21 all reproduction numbers have been  $\mathbb{R}_0 = 0.99567 < 1$ . From [6] Theorem 3.3 (4a) the implemented SIR model can have 2 endemic equilibria.

**Task 5.6** The plots for this task can be found in `sir_bed_model-t5_6.ipynb`. We have  $(S_0, I_0, R_0) = \mathbb{E}_0 = (A/d, 0, 0)$  as initial values and it is obvious that all people become susceptible individuals. First off  $S_0 = A/d$  where the count of the susceptible people is  $A$  (recruitment/birth rate of susceptible population) divided by  $d$  (per capita natural death rate). At the same time, we have no infected  $I_0$  or removed  $R_0$  individuals. Given this the initial state is disease free. Furthermore, the reproduction rate as defined in the previous section is  $\mathbb{R}_0 < 1$ . Hence we know from [8] section 3 that "on average an infected individual produces less than one new infected individual over the course of its infectious period, and the infection cannot grow".

Therefore the disease-free equilibrium  $\mathbb{E}_0 = (A/d, 0, 0)$  being an attracting node means that the trajectories in the dynamic system will move to this state. If we look at the figures in 23(a), we observe all points gathered at the equilibrium  $\mathbb{E}_0$  and given the initial values there are no infected and removed people in 23(b).

Similarly, for  $(S, I, R)$  values close to  $\mathbb{E}_0$  we assume that all trajectories will lead to this disease-free equilibrium. When performing further testing for  $(S, I, R)$  values close to  $\mathbb{E}_0$  we can verify that all trajectories lead to the disease-free equilibrium as seen in Figure 24(a) to (c). But in Figure 24(d) to (f) we can also see that Hopf bifurcation can still occur given specific values. We can verify that  $\beta > d + \nu + \mu_0$  holds in our simulations. We thus know from [6] theorem 3.3 that  $\mathbb{E}_0$  is not globally asymptotically stable, hence bifurcations seen in 24(d)-(f) are still possible.

Figure 23: Plots of disease-free equilibrium  $\mathbb{E}_0 = (A/d, 0, 0)$ Figure 24: Trajectories of  $b = 0.022$  and  $(S_0, I_0, R_0)$  close to  $\mathbb{E}_0 = (A/d, 0, 0)$

**Task 5.7: Bonus** For this task the code can be found in the python notebook `sir_bed_model-t5_7.ipynb`. Before we start with the tests we can take note from section 4 Bifurcations in [6]. It is shown that the SIR model from [6] can undergo the multiple kinds of bifurcations such as:

- Forward bifurcation
- Backward bifurcation
- Pitchfork bifurcation
- Saddle-node bifurcation
- Hopf bifurcation
- Cusp type of Bogdanov–Takens bifurcation

We have previously visualized Hopf bifurcation and in the following we will try to replicate a pitchfork bifurcation. As stated in [6] Theorem (4.1) we are considering  $\mathbb{R}_0$  as bifurcation parameter. The proof below the theorem further states that due to the definition of  $\mathbb{R}_0$  we can use  $\mu_1$  as bifurcation parameter without loss of generality. Then the necessary conditions for a pitchfork bifurcation to occur are namely the following:

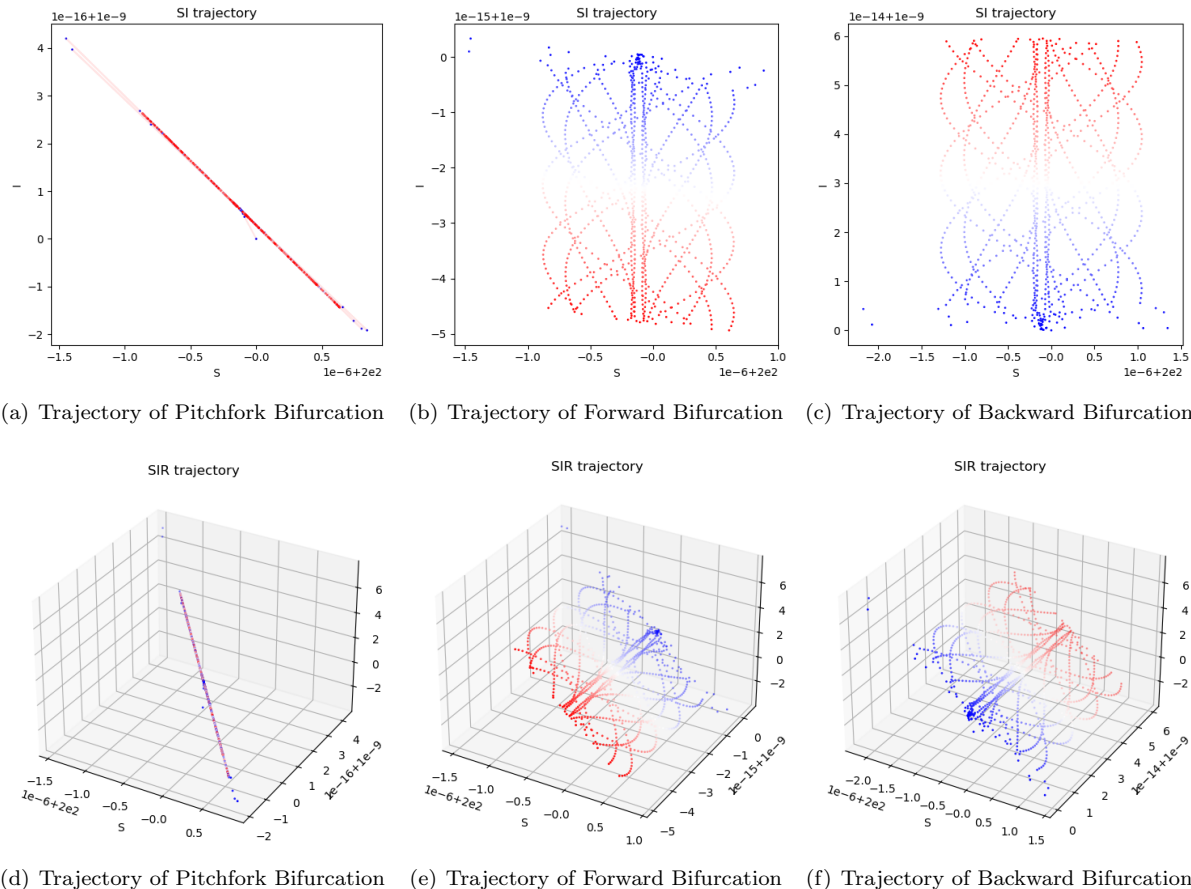
$$\begin{aligned}\mu_1 &= \beta - d - \nu + \epsilon \\ b_{pitchfork} := b &= \frac{A(\mu_1 - \mu_0)}{\beta(\beta - \nu)}\end{aligned}$$

For better comparison we also decided to additionally visualize forward and backward bifurcations. According to theorem 4.1 (1) these are respectively obtained when  $b > \frac{A(\mu_1 - \mu_0)}{\beta(\beta - \nu)}$  and  $b < \frac{A(\mu_1 - \mu_0)}{\beta(\beta - \nu)}$  holds. All parameters are set as given for task 5.3 with exception of the following. In previous iterations of the notebook the initial values  $(S_0, I_0, R_0)$  have led to interesting plots, hence these initial values will be used across all experiments. Since  $b$  can be chosen arbitrarily we have decided to use similar values as in the paper [6] Figure 7 (a) and (b), so that we can potentially obtain similar plots as in the paper. These use  $b = 0.07$  for forward bifurcation and  $b = 0.04$  for backward bifurcation.

In figures 25(d)(e)(f) we see their trajectories of each bifurcation when plotting in 3d. Since  $R$  axis is not relevant it is easier to analyse the trajectories in the  $(S, I)$  plane. This can be seen in 25(a)(b)(c). Note that the color gradient describes the change of the  $(S, I, R)$  values over time  $t$ . Here  $t = 0$  is blue and turns white and then into red when reaching the end  $t = t_{max}$ .

Figure 25(a) and (d) are the trajectories of the pitchfork bifurcation and unfortunately it is very hard to interpret it. But if we look at the trajectories of the forward (Fig. 25(b)(e)) and backward bifurcation (Fig. 25(c)(f)) we can see their similarities as well as their polar behaviour. The opposite development of their trajectories can be simply explained from their relation to the variable  $b$ . For 25(b) we could form a correlation that the amount of hospital beds  $b > b_{pitchfork}$  leads to a decrease of infected over time (indicated by the coloring) given that the reproduction number is fixed as  $\mathbb{R}_0 = 1$ . Similarly observed in 25(c)  $b > b_{pitchfork}$  In infected show an increase behaviour over time. When observing 25(b)(c) from the perspective of  $S$ , we observe periodic behaviour. This probably captures the constant, but fluctuating behaviour of the birthrate for  $S$ . Additionally we can speculate the the existence of this periodic behaviour is what causes Hopf bifurcations.

Combining previous observations we can assume that the pitchfork bifurcation in 25(a) is the point between forward and backward bifurcation, when it comes to their trajectories. This is further more expanded when observing their trajectories in 3d 25(d)-(f). We can confirm this behaviour when checking [6] Figure 2, where the point  $K$  lies between the sets of values  $C_0^+$  and  $C_0^-$ , which represent the  $(\mu_1, b)$  tuples when forward and backward bifurcations occur.

Figure 25: Trajectories in  $S, I$  and  $S, I, R$  plane

Since the trajectories can not paint the full picture, we will next look at their bifurcation diagrams. This idea is inspired by [6] Figure 7, since reproducing similar diagrams would confirm that we have plotted the pitchfork bifurcation correctly. In figures 26(a)(b)(c) the reproduction number  $\mathbb{R}_0$  is plotted against  $I$ . Note that  $\mathbb{R}_0$  is treated as bifurcation parameter, but the implementation only changes  $\mu_1$ , affecting  $\mathbb{R}_0$  in consequence. Since  $\mu_1$  is the bifurcation parameter we need to recalculate the number of infected  $I$  every time.

For better understanding of plotting  $\mathbb{R}_0$  against  $I$  we also plotted it in 3d against  $t$  in figures 26(d)(e)(f). When excluding small  $t$ -values we can confirm that bifurcation diagram is consistent across all time slices.

The initial observation is that all bifurcation diagrams look similar. We can easily confirm that 26(b) is behaving as expected, when comparing it to [6] Figure 7(a). In a forward bifurcation, as the bifurcation parameter crosses a critical threshold, the system transitions from one stable state to another. Before the threshold we are in the disease-free equilibrium and afterwards the onset of the epidemic is seen as  $\mathbb{R}_0$  crosses the threshold of 1.

As for backward bifurcation Figure 7(b) from [6] shows that the existence of an epidemic extends also for some values below  $\mathbb{R}_0 < 1$ . While 26 does not fully capture this (due to implementations haven't taken too long up to this point), we can see that the cut-off at  $\mathbb{R} = 1$  implies this behaviour of the backwards bifurcation.

When looking at 26(a) we can note that the bifurcation diagram is likely the same as the forward bifurcation. We can say at this point that like the forward bifurcation, the pitchfork bifurcation marks the start of an epidemic as well, when crossing  $\mathbb{R}_0$ . Unfortunately the pitchfork bifurcation does not show the characteristic pitchfork shape. Logically speaking it wouldn't make sense to observe a decrease in infected individuals given that there is none, while increasing the reproduction number crossing the threshold  $\mathbb{R}_0 = 1$ . Looking back into [6] the proof of theorem 4.1 shows that the set of points describing pitchfork bifurcations can be described using the following:

$$C_{\Delta}^{\pm} : b = f_{\Delta}^{\pm}(\mu_1) \triangleq \frac{\beta(\mu_1 - \mu_0) + \delta_0(\delta_1 - \beta) \pm \sqrt{\beta\delta_1(\mu_1 - \mu_0)(\delta_1 - \beta)}}{(\beta - \nu)\delta_1^2}$$

$$\delta_0 = d + \nu + \mu_0$$

$$\delta_1 = d + \nu + \mu_1$$

It can then be verified that then  $f_{\Delta}^{\pm}(\delta - d - \nu) = \frac{A(\mu_1 - \mu_0)}{\beta(\beta - \nu)}$  holds. This is verified in the python notebook as well using the functions `f_plus(...)` and `f_minus(...)`. This explains why the pitchfork bifurcation in  $\mathbb{R}_0, I$  plane shows the same behaviour as the forward bifurcation. The observe characteristic we would probably instead need to plot  $b$  against  $\mu_1$  using the definition  $b = f_{\Delta}^{\pm}(\mu_1)$ . The curves of  $C_0^+$  and  $C_0^-$  could be interpreted as the pitchfork.

Overall we can see that SIR model described using the differential equations in [6](2.2) is a very complex dynamical system. In this task have observed that different bifurcations can occur given the right settings. As for the pitchfork bifurcation it exists under special conditions such that the forking part overlaps with each other.

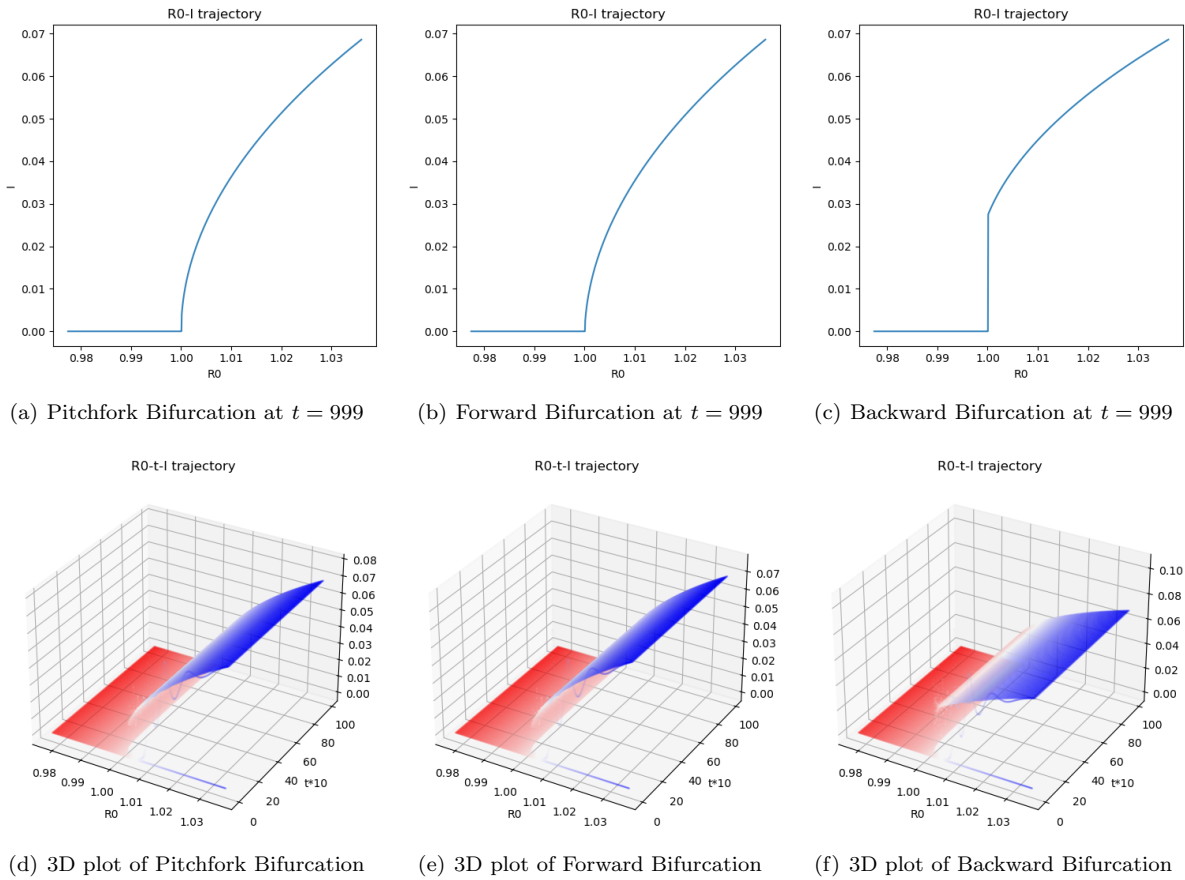


Figure 26: Bifurcation diagram on  $\mathbb{R}_0, I$  plane

## References

- [1] James Gleick. *Chaos: Making a new science*. Penguin, 2008.
- [2] Morris W Hirsch, Stephen Smale, and Robert L Devaney. *Differential equations, dynamical systems, and an introduction to chaos*. Academic press, 2012.
- [3] Yuri A. Kuznetsov. *Elements of applied bifurcation theory*. Number 112 in Applied Mathematical Sciences. Springer, Berlin, 2 edition, 1998.
- [4] Edward N Lorenz. Deterministic nonperiodic flow. *Journal of atmospheric sciences*, 20(2):130–141, 1963.
- [5] Prof. Rudolfo Rosales. Hopf bifurcations, Dec. 13, 2023 [Online].
- [6] Chunhua Shan and Huaiping Zhu. Bifurcations and complex dynamics of an sir model with the impact of the number of hospital beds. *Journal of Differential Equations*, 257(5):1662–1688, 2014.
- [7] Steven H Strogatz. *Nonlinear dynamics and chaos with student solutions manual: With applications to physics, biology, chemistry, and engineering*. CRC press, 2018.
- [8] Pauline Van den Driessche and James Watmough. Reproduction numbers and sub-threshold endemic equilibria for compartmental models of disease transmission. *Mathematical biosciences*, 180(1-2):29–48, 2002.